RFID-Based Reconfigurable Electromagnetic Devices

Francesco Lestini, *Student Member, IEEE,* Gaetano Marrocco, *Senior Member, IEEE,* and Cecilia Occhiuzzi, *Member, IEEE*

***Abstract*—Modern wireless communication systems are becoming increasingly necessary, emphasizing the need for electromagnetic devices that can flexibly operate under different conditions, e.g., under power constraints or in hostile environments where scattering objects randomly modify coverage areas and communication links. Due to their ability to dynamically change operating frequency, radiation pattern, bandwidth characteristics, and polarization, reconfigurable objects (especially antennas and backscattering surfaces) have received significant attention in this context. Electromagnetic features can be electronically selected by controlling the bias voltage of tunable elements adequately integrated into the layout. Usually, this is done by employing external programmable controllers that need power sources and wired connections, leading to unusable configurations for several scenarios. Thus, exploring alternative electronic tuning mechanisms becomes essential. This paper proposes RFID-Based Reconfigurable Electromagnetic Devices as a wireless, cost-effective, and low-power solution. The system's operating principle, potential architectures, and applicability in practical scenarios are presented. Theoretical and experimental analysis validate the proposed architecture, whose capabilities are finally demonstrated by prototyping and testing two reconfigurable antenna arrays.**

***Index Terms*—RFID, reconfigurable devices, remote control, low power consumption.**

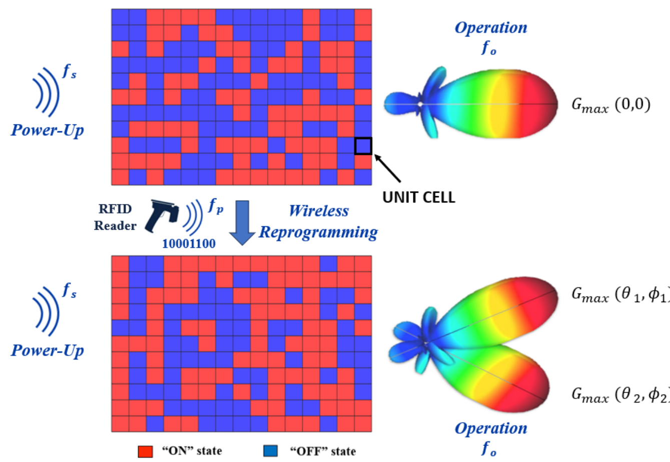

Fig. 1. Concept of RFID-Based wireless programmability of a grid of reconfigurable elements. A generic electromagnetic signal at f_s powers up the grid. According to the configuration stored in the IC_i memory, RF elements $Z_{i,n,m}$ are enabled or disabled, thus changing the state of unit cells of the grid, and consequently, an operative feature at f_o (in the example a radiation pattern). A reconfiguration can change the layout through an RFID reader operating at f_p, and different radiation patterns can be obtained.

I. Introduction

IN recent years, the need for advanced wireless communication systems and the rapid expansion of the Internet of Things (IoT) applications have highlighted the necessity for electromagnetic devices that can quickly adapt to a wide range of operating conditions [1], [2]. In this scenario, reconfigurable objects have attracted notable attention due to their ability to dynamically change operating frequency, radiation pattern, polarization behavior, or a combination of them [3]. Examples of reconfigurable devices are stand-alone radiating elements [4], [5], antenna arrays [6], [7], Frequency Selective Surfaces (FSSs) [8], [9], and Reconfigurable Intelligent Surfaces (RISs) [10], [11].

An Electromagnetic (EM) device can be reconfigured by redistributing its surface currents in a controllable way to induce modifications in its fundamental electromagnetic features. This can be done by singularly or jointly exploiting mechanical, all-electronic, material-based, and optical methods [12]. Electrical-based reconfigurability [13] can be achieved by loading the device with electrically tunable components such as PIN diodes, Micro-Electro-Mechanical Systems (MEMS) switches, or varactor diodes, whose bias voltage can be adjusted by using programmable controllers such as Field Programmable Gate Arrays (FPGAs) or Digital Signal Processors (DSPs) [14]–[16]. However, the widespread use of reconfigurable devices is currently prevented by the required power, high cost, and complexity of programmable controllers [17], the need for additional elements such as shift registers, and the physically wired interconnections required to connect the entire reconfiguration network. This is especially a problem for some kinds of applications, like body-worn antennas or devices embedded in buildings, materials, or moving objects [18]–[20], for which wired interconnections are particularly difficult to implement.

In this paper, we propose a wireless reconfiguration architecture based on the Ultra-High-Frequency Radio Frequency Identification (UHF RFID) technology since it is low-cost, low-power, and capable of providing wireless connectivity and basic computational capabilities through simple and miniaturized devices [21]. The rationale for this approach is that the latest generation of RFID Integrated Circuits (ICs) [22], [23] can also act as a DC power supplier for external devices [24], having a DC port whose voltage can be set as a reply of a command sent directly by the reader or stored in their

The authors are with the Pervasive Electromagnetics Lab, University of Rome Tor Vergata, Via del Politecnico 1, Rome 00133, Italy. (email: francesco.lestini@uniroma2.it, gaetano.marrocco@uniroma2.it, cecilia.occhiuzzi@uniroma2.it).

internal memory bank [25]. Therefore, the idea is to combine the *digital features* of the ICs typically embedded in RFID transponders with the *analog features* of classical electromagnetic devices to provide them with *wireless reconfigurability*. RFID ICs thus become wireless controllers (Fig. 1), enabling the removal of power supplies, cables, and expensive programmable devices that are required by traditional wired reconfigurable architectures.

The idea to use RFID technology as a reconfigurable platform was preliminary introduced in [26], where authors demonstrated the possibility of assisting a source-destination link by forcing RFID tags composing a RIS to backscatter in carefully selected groups. The control of tags' behaviour was only at the protocol level, without modifying the layout of the surface. In [27] instead, a preliminary attempt of using tags to control tunable elements embedded into a reflective surface was presented. An 8x8-element information metasurface was introduced, in which RFID tags were used to achieve beam splitting, beamforming, and EM-wave absorption of the surface. The Authors recently presented in [28] an early feasibility evaluation of the proposed approach. An arrangement of two elements operating in the RFID UHF band was configured to turn communication on or off with the external reader selectively. This paper extends these results to describe better architectures, operating principles, possibilities, and limitations concerning real-world applications. For this purpose, the IC performance in different frequency bands is characterized to evaluate the possibility of exploiting the proposed architecture with different electromagnetic sources outside the typical UHF RFID frequency band and, hence, to analyze the usability in supporting other communication platforms and services.

The paper is organized as follows: in Section II, we provide a detailed description of the rationale of the proposed approach, the operative architectures, the potentialities, and the constraints. Section III characterizes the IC programmability features, with particular attention to typical electromagnetic environmental sources, such as LoRa, WiFi, Bluetooth, and sub-S 5G communications. Then, preliminary proofs of the proposed wireless reconfigurability are provided in Section IV through two application examples. In the first, the selective activation of an RFID tag depending on the state of another one is demonstrated. In the second case, the radiation pattern of a 3-elements array is configured to switch between directive and omnidirectional radiation modes.

II. Rationale

The principle of the proposed reconfiguration method is sketched in Fig. 2. For clarity, we focus on an electromagnetic object (EM-O) made up of only three conductive elements (namely *a, b, c*), whose mutual connections are determined by the state of an RF switch ($Z^{ON,OFF}$), adequately controlled by the RFID IC. The described architecture can be easily extended to a generic grid of $n \times m$ unit cells, integrating one or more RF components ($Z_{i,n,m}^{ON,OFF}$), and adequately controlled by one or more RFID IC_i (see Fig. 1 again). The resulting structure will be provided with *i-bit reconfigurability* since a single RFID IC can control several switches, but not independently.

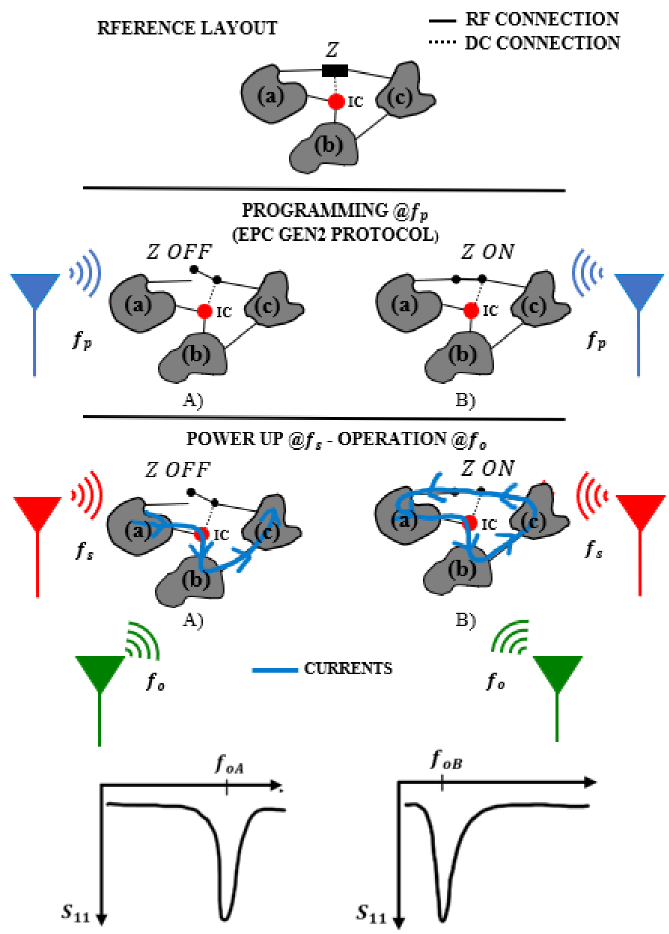

Fig. 2. Rationale of the proposed RFID-Based Reconfigurable Electromagnetic Object. The reference layout consists of three conductive elements (*a, b, c*) properly connected to an RFID IC. The latter controls the state of a tunable element ($Z^{ON,OFF}$) through its DC output ports, thus determining the configuration assumed by the object and its electromagnetic features.

During *programming* phase, multiple configurations can be imposed (as *A, B* in the example) corresponding to different arrangements of the three unit cells. Programming is achieved using EPC UHF Gen2 commands [29] sent by an RFID reader at the UHF frequency f_p and stored in the internal writable and non-volatile memory of the IC (Fig. 2, *Programming*). When a compatible RF field at frequency f_s and power P_{harv} impinges upon the layout (Fig. 2, *Power-up*), the IC can be activated provided that $P_{harv} \geq p_c$, the power required to activate its circuitry at the source frequency f_s. Subsequently, the RFID IC drives the RF switch to which it is connected depending on the command stored in its internal memory. The layout will hence assume one of the preset configurations (A or B), modifying the currents flowing through the EM-O and its electromagnetic characteristics, i.e., its operative frequency f_o, bandwidth, radiation pattern, and polarization (Fig. 2, *Operation*). The activation field at f_s can be modulated or not, meaning that alternative ambient sources, such as Wifi, Bluetooth, cellular network signals, or even pure ad-hoc sinusoidal fields, can be utilized [30]. However, the activation field must continuously illuminate the EM-O throughout its operation to benefit from the programmed configuration.

TABLE I
FREQUENCIES, FIELDS, AND OPERATION OF THE RECONFIGURABLE EM-O

Action	Frequency	Field
Programming	f_p	EPC UHF Gen2 command
Power-up	f_s	Generic modulated/unmodulated signal
Operation	f_o	Operative field of the EM-O

A. Operation and Architectures

Three working conditions can be identified, each with its frequency and required/produced signals as specified in Table I :

1) *Programming:* The desired RF component status ($Z^{ON,OFF}$) is stored in the IC user memory. The RFID Gen2 protocol [29] must be used.
2) *Power-up:* When a compatible RF source illuminates the IC, it will deliver or not a DC voltage to the connected RF component, depending on the imposed state.
3) *Operation:* While illuminated, the EM-O performs actions according to the imposed configuration.

The power-up and operation phases are dependent and synchronous. Programming can be performed, instead, offline and repeated several times, depending on the particular application. The RFID-based programmable EM-O is an inherently multi-frequency device, capable of operating at the three different frequencies $f_p,\ f_s,\ f_o$. Two architectures can be envisaged:

1) The ICs are embedded directly in the layout so that the same conductive elements seamlessly do harvest, activation, and operation;
2) Harvest, activation, and operation are demanded to specific layout portions, each tuned to the particular frequency $f_p,\ f_s,\ f_o$. In this perspective, it is possible to properly include in the device *Programming* and *Operating nodes* whose relationship can be assumed to be similar to the typical *master/slave* one.

According to the chosen configuration, the requirements on multi-frequency behavior could be relaxed in case power-up, operation, and programming rely on the same bandwidth/service ($f_s = f_p = f_o$) as it is for systems conceived only for RFID applications.

III. IC CHARACTERIZATION

In the most general case, the *power-up* and *operation* frequencies and the signals listed in Table I can differ from those foreseen by the UHF EPC Gen2 protocol. Although some experimental evidence [30] suggested that RFID ICs can also operate in other frequency bands, the nominal features are generally available from the datasheet only in the UHF band. Thus, to evaluate the real possibility of exploiting ambient sources to power-up the reconfigurable device, the power sensitivity $p_c(f)$ at different frequencies needs to be characterized. Furthermore, to select the most suitable RF switch to be integrated into the layout, the DC power output V_{out} must be evaluated regarding absolute values and stability.

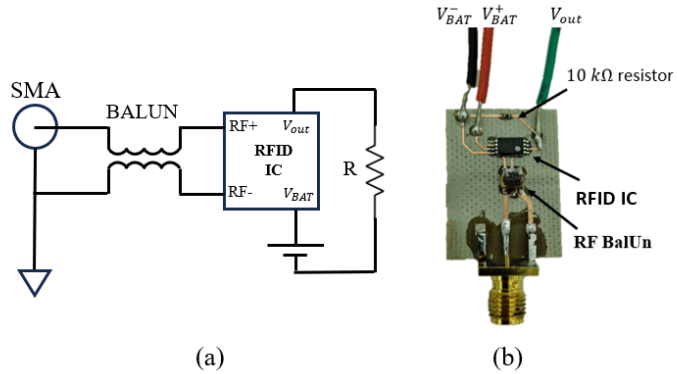

Fig. 3. Board for IC characterization. (a) Schematic representation of DUT connections. (a) Custom fabricated fixture for IC characterization.

To cover the most common ambient sources (listed in Table II), a broadband analysis was conducted within the $0.4\ GHz - 5\ GHz$ frequency band through a custom board (Fig. 3.b) implementing the procedure described in [31]. The board connects the IC to a Vector Network Analyzer (VNA) for sensitivity characterization over frequency $p_c(f)$ and to a digital multimeter for measuring the DC voltage output V_{out}. An RF-BalUn [32] was included between the IC RF ports and the VNA for pre-matching and balancing purposes [31] while a $10\ k\Omega$ resistor was connected to the output port to perform voltage measurements. After a first calibration phase through a custom Short-Open-Load (SOL) calibration kit, by exploiting the wired *turn-on* method [33], VNA measures the reflection coefficient S_{11} when it feeds the IC at different frequencies with increasing power P_{VNA}. The amount of power that actually reaches the IC ($P_{\text{on-chip}}$) depends on the S_{11} as follows:

$$P_{\text{on-chip}} = P_{\text{VNA}}\left(1 - |S_{11}|^2\right) \tag{1}$$

When $P_{\text{on-chip}} = p_c$ the IC activates and an abrupt change in the measured S_{11} is observed [31]. Consequently, the voltage level of the DC output port starts arising, and the p_c can be extracted from the measured S_{11} and P_{VNA}.

A. Measurement Results

To our knowledge, only two commercially available ICs, the EM4152 [22] and the EM4325 [23], provide the required feature of a controllable DC output port. This paper relies on the characterization of the EM4325 IC ($Z_{chip} = 7.6 - j114\ \Omega$, $p_c = -31\ dBm$), which operates in Battery Assisted Passive (BAP) mode, which means that the supply of the external component is provided by the battery ($V_{out} = 3.3\ V$). A VNA [34] operating in the frequency band $f_s = 0.4 - 5\ GHz$ and with a power level P_{VNA} ranging from -20 dBm to 10 dBm was used. The results are visible in Fig. 4 and Fig. 5. Being the EM4325 operating in BAP mode, the sensitivity was approximately $p_c = -31\ dBm$ up to around $f_s = 1\ GHz$ (Fig. 4), coherently with the datasheet. Then, a sharp and monotonic increasing trend was measured, meaning that the IC performs worse when operating far from the UHF band, and the benefits of the battery strongly degrade, at least for

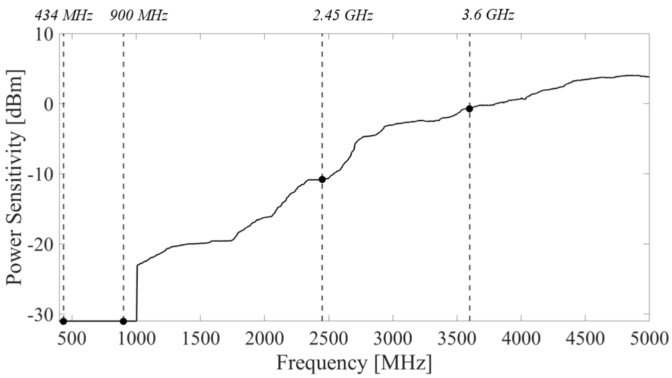

Fig. 4. Measured power sensitivity of EM4325 over frequency.

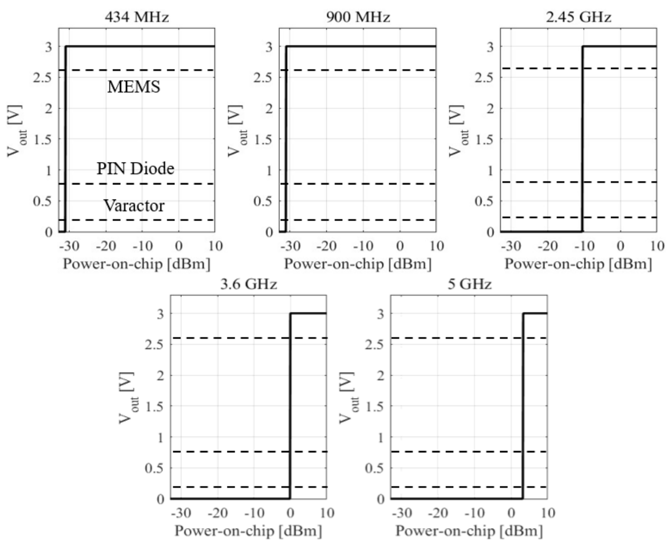

Fig. 5. Output DC voltage delivered by the EM4325 IC versus power-on-chip at different frequencies. Dashed lines indicate the threshold voltages for MEMS, PIN diodes, and varactor diodes.

the power-up. It is worth noticing that, up to 2.45 GHz, p_c aligns with standard ICs operating in the UHF band.

The DC output voltage V_{out} versus the power-on-chip $P_{\text{on-chip}}$ is visible in Fig. 5 for the set of frequencies listed in Table II. Since the external battery provides the output voltage, the EM4325 only needs to be turned on to achieve the maximum DC output V_{out}^{max} (Fig. 5), which depends only on the battery capabilities (up to 3.3 V [23]). Moreover, once V_{out}^{max} is reached, the output is stable and free of oscillations, damping, or drift.

B. Discussions

The measured operative sensitivities can be exploited to theoretically derive the maximum operating distances for a hypothetical reconfigurable EM-O integrating the previously mentioned IC. By considering ambient RF sources (whose Emission Power Levels (EPLs) are imposed by the Federal Communication Committee (FCC) and the European Telecommunications Standards Institute (ETSI)) under the hypothesis of polarization matching between the RF emitter and the reconfigurable EM-O and a realized gain of 0 dBi for both the

TABLE II
MAXIMUM ALLOWED ACTIVATION DISTANCES FOR THE SELECTED IC.

Frequency	Service	EPL [dBm]	$\mathbf{d_{max}}$ [m]
434 MHz	EU433 LoRa	10	3
900 MHz	UHF RFID	30	13.5
2.45 GHz	Wi-Fi, Bluetooth	20	1
3.6 GHz	5G mid-band	23	0.35
5 GHz	Wi-Fi, Bluetooth	23	0.05

TABLE III
RF TUNABLE ELEMENTS

Type	Threshold [V]-[A]	Note
PIN diode	0.6-0.8 V/0.1-1 mA	High Power
MEMS Switch	2.5-3.3 V/1-10 μA	Low power
Varactor diode	0.2V/1-10 nA	Voltage stability required

receiver and the transceiver, the maximum activation distance can be calculated as [35]:

$$d_{\max} = \frac{c}{4\pi f}\sqrt{\frac{EPL}{p_o}}, \tag{2}$$

where c is the speed of light, and f_o and EPL are the frequency and the maximum emission power level of the considered RF source, respectively. The resulting maximum allowed distances are listed in Table II and highlight that the IC can operate up to 1 m with 2.45 GHz Wi-Fi or Bluetooth signals. In contrast, the activation distance reduces to only a few centimeters at 5 GHz. This result suggests that, for higher frequencies, a dedicated RF source would be needed.

Regarding the type of tunable elements, it is possible to state that varactors, MEMS switches, and PIN diodes would be suitable for BAP ICs, since the maximum value of V_{out} is stable, reached instantaneously, and compatible with the switching thresholds of the above-mentioned tunable components (as outlined by the features listed in Table III).

IV. PRELIMINARY FEASIBILITY EXAMPLES

In this section, we provide two feasibility examples to demonstrate the reprogramming capability of the proposed architecture in terms of the selective activation of antenna nodes and the beam shaping of a 3-element array. For the sake of simplicity, all three operating steps of Section II (programming, power-up, and operation) were carried out at 900 MHz.

A. Selective Activation of Nodes

A first example considered the EM4325 to realize a two-node system, in which a programming node controls the communication capability of an operating node. For the sake of simplicity, here $f_p = f_s = f_o = 900\,MHz$. The programming node can be seen as a *wireless security token* (i.e., a device that is used in addition to, or in place of a password to gain access to another device [36]) for the operating node, which can be, for example, an RFID sensor.

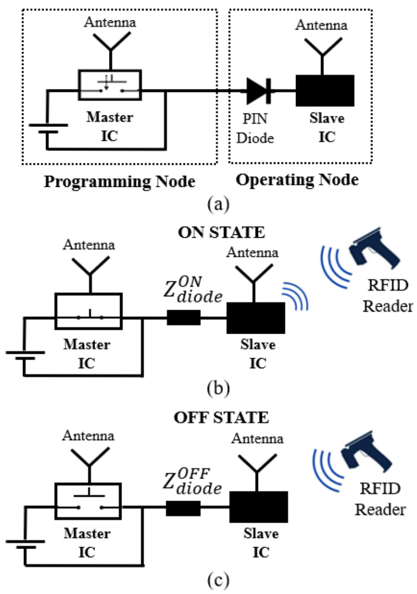

Fig. 6. (a) Schematic representation of layout for selective activation of RFID nodes. (b) When activated, the master IC sets the diode impedance to Z_{diode}^{ON}, enabling the slave IC to respond to an RFID interrogation. (c) When the master IC is in the off state, the diode impedance is changed to Z_{diode}^{OFF}, causing the slave IC to stop responding.

The programming node is equipped with the EM4325 IC (*master IC*), while the operating node integrates a Magnus S3 IC (*slave IC*) ($Z_{chip} = 7.6 - j114\ \Omega$, $p_c = -16\ dBm$ [37]) and a PIN diode (Fig. 6). The aim is that the slave IC can be enabled or not, depending on the state of the master IC. Indeed, when the master IC is powered up and its DC output port is activated, the diode impedance is set to Z_{diode}^{ON}, allowing the slave IC to respond to an RFID interrogation. On the other hand, when the DC output port is deactivated, the diode impedance is set to Z_{diode}^{OFF} even if the master IC is powered up, causing the slave IC to stop responding.

The programming and operating nodes were realized as two dipoles, orthogonally arranged for coupling minimization purposes (Fig. 7). The ICs were matched to their respective antenna impedance through a T-match [35] and the PIN diode [38] was connected to the DC output pin of the master IC and the T-match of the slave IC so that, by changing the state of the master IC, a substantial variation of the current flowing on the T-match can be imposed. More specifically, when the diode is off, its impedance resembles an open circuit, leading to a complete mismatch of the operating tag and its inactivation. In contrast, when the diode is on, the operating tag results matched and capable of replying to the RFID interrogation. Finally, ferrite beads [39] were also integrated with the layout for both dipoles to decouple them from the 3.3 V DC voltage of the battery.

Preliminary simulations of the system were performed using CST Microwave Studio 2023. The dipoles were printed on a 1.6 cm thick FR-4 substrate ($\varepsilon_r = 4.3$, $tan\delta = 0.025$), and the PIN diode was simulated through its .s2p file. Geometrical parameters (Fig. 7) were optimized to achieve the behavior described in Fig. 6. Indeed, when the PIN diode is on, the impedance matching is achieved (power transmission coeffi-

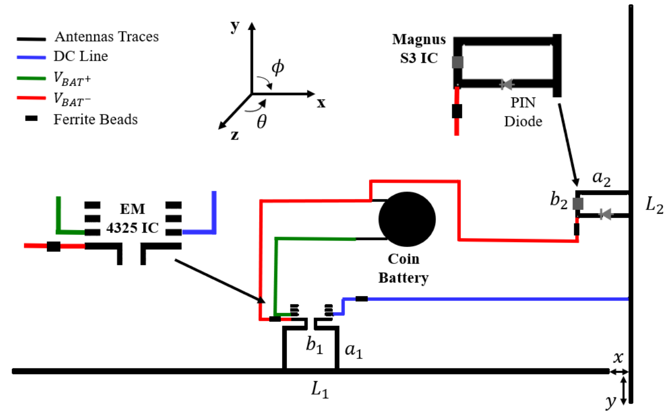

Fig. 7. Layout of the 2-element RFID system. Geometrical dimensions: $L_1 = 100\ mm$, $a_1 = 6\ mm$, $b_1 = 7.5\ mm$, $L_2 = 70\ mm$, $a_2 = 7.5\ mm$, $b_2 = 3\ mm$, $x = 3\ mm$, $y = 5\ mm$.

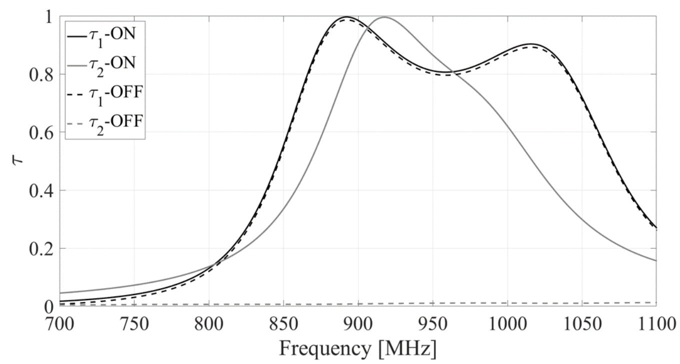

Fig. 8. Simulated power transfer coefficients τ for the two dipoles, in ON and OFF state.

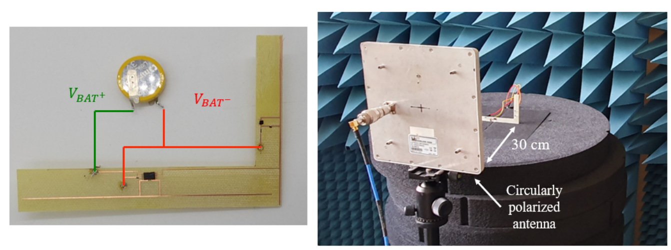

(a) (b)

Fig. 9. (a) The fabricated prototype. (b) Measurement setup.

cient [35] $\tau_1 = 0.98$, $\tau_2 = 0.9$), while when it is switched to its off state, the slave IC is mismatched ($\tau_2 = 0.08$), as illustrated in Fig. 8.

Measurements were performed with a prototype that was realized by etching copper from an FR-4 Printed Circuit Board (PCB) using a milling machine, while electronic components (IC, diodes, and ferrite beads) were soldered with the help of a bench soldering iron. The experimental setup (Fig. 9) consisted of a circularly polarized antenna (patch with broadside gain $G_R = 7.5\ dBic$) placed 30 cm away from the prototype and connected to the TagFormance UHF Pro station for interrogation. Realized gains were retrieved by the turn-on power method [28]. Fig. 10 compares the measured and simulated data for both antennas in both states, highlighting the good

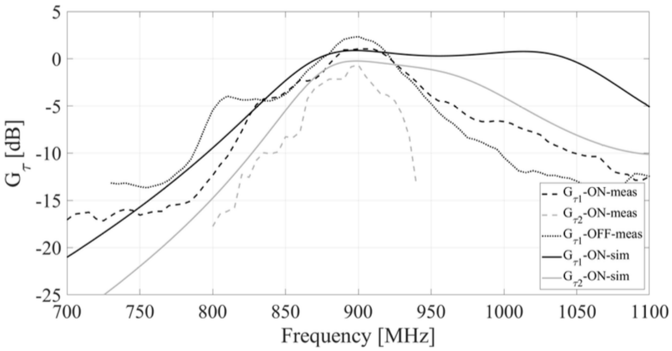

Fig. 10. Simulated and measured realized gains $G\tau$ in ON and OFF states.

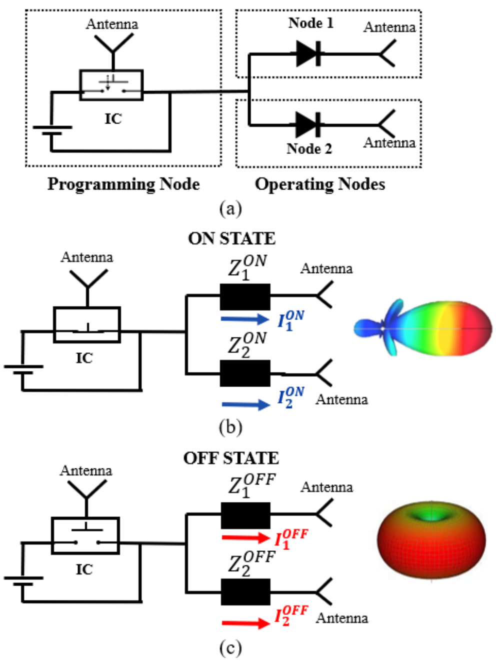

Fig. 11. (a) Schematic representation of the layout for RFID-Based wireless beam shaping. (b) When activated, the RFID IC sets the diodes impedances to Z_1^{ON} and Z_2^{ON}, imposing the flow of currents I_1^{ON} and I_2^{ON} through the operating nodes antennas. (c) On the other hand, if the IC is in the off state, the diodes impedances are changed to Z_1^{OFF} and Z_2^{OFF}, resulting in the variation of the currents flowing through the operating nodes to I_1^{OFF} and I_2^{OFF}.

agreement and the effective enabled/disabled communication with the slave IC in the different states.

B. Beam Shaping

The second experiment aims to demonstrate the beam's shaping of a 3-elements antenna array. The array comprises the programming node and two operating nodes (Fig. 11). The programming node includes EM4325 while operating nodes integrate only a PIN diode. When the IC is reprogrammed, the PIN diodes embedded in each operating node change their impedance leading to a variation in the currents flowing through their respective antennas (from I_1^{ON}, I_2^{ON} to I_1^{OFF}, I_2^{OFF} and vice versa) and thus in the radiation pattern of the whole array (Fig. 11).

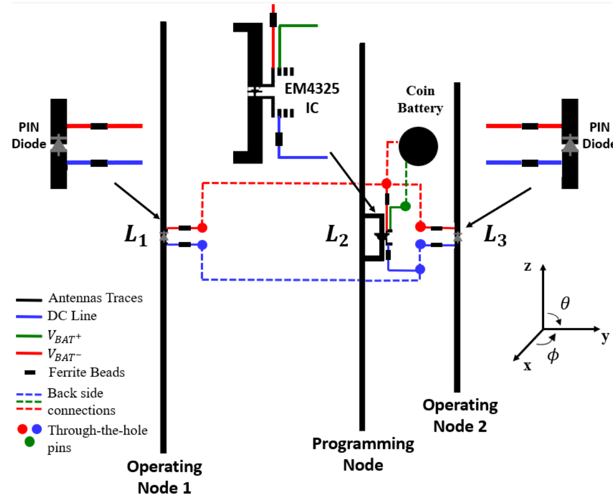

Fig. 12. Layout of the wireless reconfigurable 3-element array. Geometrical dimensions are: $L_1 = 167\ mm$, $L_2 = 150\ mm$, $L_3 = 120\ mm$. Distances among elements are: $D_{12} = 80\ mm$, $D_{23} = 38\ mm$.

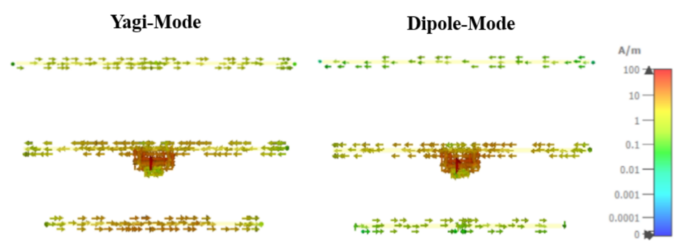

Fig. 13. Simulated surface currents (@900 MHz) flowing through the three elements in both states.

The system was designed as depicted in Fig. 12. Again, the IC impedance was matched through a T-match, and dipoles were placed on an FR-4 substrate. PIN diodes were connected to the DC output pin of the IC and the negative pin of the battery (which was placed on the back side) via ferrite beads. Geometric parameters, i.e., the lengths of the programming and operating nodes and their mutual distances, were chosen as the result of a parametric analysis oriented to optimize the realized gain G_τ of the array. The system was designed to work as follows: when the RFID IC is in the on state (*Yagi mode*) and activated, both diodes are on; hence, they ideally act as short circuits, and the typical Yagi-Uda radiation pattern is achieved. On the other hand, when diodes are switched to the off state (*dipole mode*), they act similarly to an open circuit resulting in the array radiation pattern reconfiguration to a "dipole-like" pattern. As expected, the RFID programming effectively changes the pattern of the currents of the structure, as visible in Fig. 13. Indeed, in the dipole mode operation, only weak currents flow through the passive elements, while in the Yagi mode, currents are sensibly higher.

The numerical analysis was validated by measuring the realized gain and the radiation pattern using the TagFormance UHF Pro station. The prototype is visible in Fig.14. Fig. 15 compares the array antenna's simulated and measured realized gain for both states in the end-fire direction. Measurements agree with simulations, and both highlight a notable change

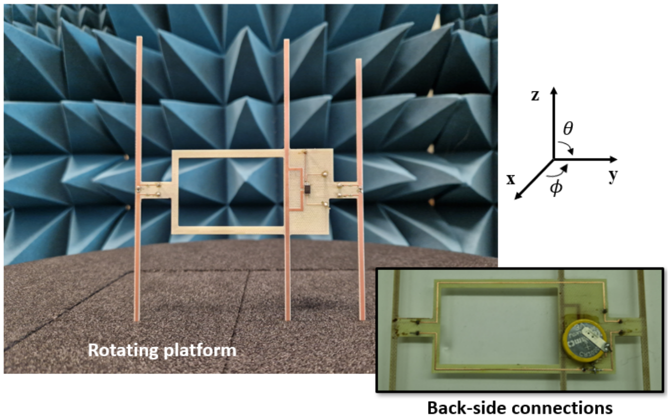

Fig. 14. Front and back view of the realized prototype placed on the rotating platforms for radiation pattern measurement purposes. Geometrical dimensions are as described in Fig. 12.

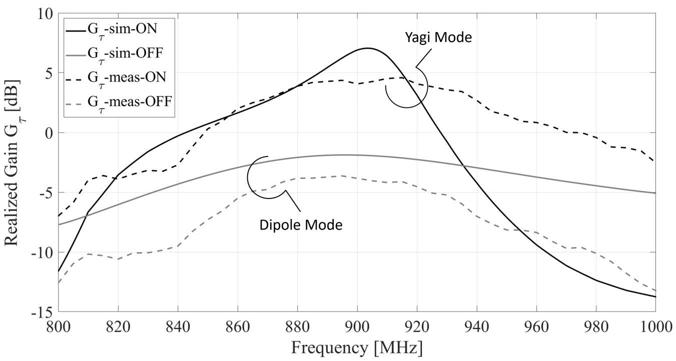

Fig. 15. Simulated and measured realized gains for the wireless reconfigurable array in both states.

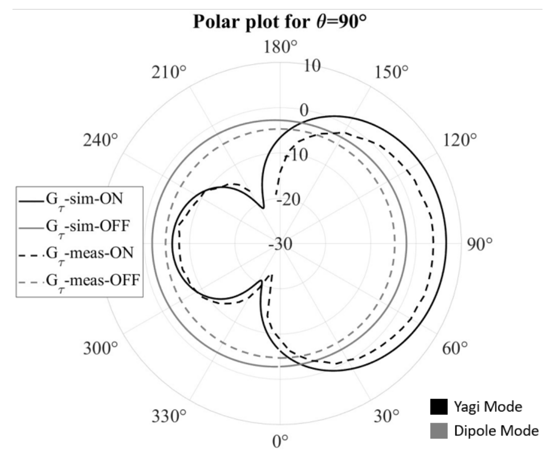

Fig. 16. Simulated and measured radiation patterns for the wireless reconfigurable array in the end-fire direction in both states.

in the gain absolute values due to the transition from the Yagi mode to the Dipole mode. Differences between simulations and measurements could be caused by uncertainties in the simulated equivalent impedance of the PIN diodes, which are highly voltage-sensitive. Finally, the measured radiation patterns are shown in Fig. 16. Also in this case, there is a good agreement with simulations, definitely proving the radiation pattern reconfiguration capabilities of the proposed system. Indeed, in the Yagi-mode, the array has an *endfire* radiation pattern with a maximum realized gain of 4 dB ($G_{\tau}^{sim,max} = 6.6\ dB$) for $\phi = 0°$ and a front-to-back ratio of about 12 dB. In the dipole mode, instead, the antenna exhibits an *isotropic* radiation pattern with a realized gain of -4.7 dB ($G_{\tau}^{sim,max} = -2.2\ dB$).

V. Conclusions

This paper introduces, discusses, and experimentally validates the idea of RFID-based wireless programmable electromagnetic objects. When compared with traditional electronic tuning mechanism in which an FPGA and several shift registers provide the bias voltage required by the tunable components [12], the proposed RFID-Based wireless programmability provides similar output voltages and currents (Table IV) and several advantages which are listed in Table IV and discussed below:

- *Reduced Power Consumption:* The power required to drive a reconfigurable electromagnetic device is composed of the *dynamic power* consumed by the tunable elements ($P_{dynamic} = N \cdot P_{switch}$, where N is the number of RF switches) and the *static power* (P_{static}) consumed by the control circuit. Typically, the power required by an FPGA is $\approx 5\ W$ [40], [17], while the RFID IC used in this paper consumes only $5 - 30\ \mu W$ from the battery [23].
- *Reduced Cost:* The cost of an FPGA is around hundreds of euros, while that of an RFID IC is less than 1 euro. However, it should be noted that a single FPGA is capable of *independently* driving hundreds of tunable components, while an RFID IC can only set one state at a time, which means that the *minimum* number of required ICs is equal to the number of desired reconfigurability bits. Therefore, the proposed approach is beneficial for all those reconfigurable devices that require a limited number of bits, as the cost is significantly reduced, while for more complex structures, the traditional reconfiguration mechanism should still be preferred.
- *Reduced Complexity:* In addition to removing physical wires, the proposed solution could also simplify the structure by eliminating the complicated biasing lines needed to drive the tunable elements. Indeed, since RFID ICs are miniaturized and lightweight components, they can be distributed across the reconfigurable EM-O, reducing the length and number of required biasing lines and thus limiting unwanted interference, losses, and radiation pattern distortion. Moreover, the device can also be made flexible and deployable in all those environments where cables are not allowed.

However, the RFID-Based wireless reconfiguration mechanism also presents some limitations and challenges that need to be addressed, especially considering reconfigurable EM-O operating at higher frequencies. For instance, the IC characterization has highlighted that the IC sensitivity p_c, and thus the activation distance d_{max}, degrade as the frequency f_s

TABLE IV
COMPARISON OF THE PROPOSED APPROACH WITH THE STATE-OF-THE-ART FPGA-BASED ELECTRONIC TUNING MECHANISM. THE TECHNICAL DETAILS ARE FROM A STANDARD COMMERCIAL FPGA [40].

Reconfiguration Mechanism	Output Characteristics	Power Consumption	Cost
Electrical	V_{out} up to 3.3 V I_{out} up to 24 mA	$P_{static} \approx 5\ W$ $P_{dynamic} = N \cdot P_{switch}$	$FPGA \approx 200$ € $Shift\ Register \approx 1$ € (each)
RFID-Based	V_{out} up to 3.3 V I_{out} up to 20 mA	$P_{static} \approx 0\ W$ $P_{dynamic} = N \cdot P_{switch}$	$RFID\ IC \approx 1$ € (each)

increases, pointing out that it could be necessary to include a dedicated RF source in the system architecture, thereby reducing the benefits of reduced complexity discussed above.

Future activities will be devoted to characterizing the feasibility of adopting a pure passive configuration for battery removal and validating activation and operation through different ambient sources.

REFERENCES

[1] A. Jabbar, M. A. Jamshed, Q. Abbasi, M. A. Imran, and M. Ur-Rehman, “Leveraging the role of dynamic reconfigurable antennas in viewpoint of industry 4.0 and beyond,” *Research*, vol. 6, p. 0110, 2023.

[2] C. G. Christodoulou, Y. Tawk, S. A. Lane, and S. R. Erwin, “Reconfigurable antennas for wireless and space applications,” *Proceedings of the IEEE*, vol. 100, no. 7, pp. 2250–2261, 2012.

[3] J. Costantine, Y. Tawk, S. E. Barbin, and C. G. Christodoulou, “Reconfigurable antennas: Design and applications,” *Proceedings of the IEEE*, vol. 103, no. 3, pp. 424–437, 2015.

[4] M. Li, Z. Zhang, M.-C. Tang, L. Zhu, and N.-W. Liu, “Bandwidth enhancement and size reduction of a low-profile polarization-reconfigurable antenna by utilizing multiple resonances,” *IEEE Transactions on Antennas and Propagation*, vol. 70, no. 2, pp. 1517–1522, 2021.

[5] U. Musa, S. M. Shah, H. A. Majid, Z. Z. Abidin, M. S. Yahya, S. Babani, and Z. Yunusa, “Recent advancement of wearable reconfigurable antenna technologies: A review,” *IEEE Access*, vol. 10, pp. 121 831–121 863, 2022.

[6] D. Piazza, N. J. Kirsch, A. Forenza, R. W. Heath, and K. R. Dandekar, “Design and evaluation of a reconfigurable antenna array for mimo systems,” *IEEE Transactions on antennas and propagation*, vol. 56, no. 3, pp. 869–881, 2008.

[7] Y. Wang, F. Xu, Y.-Q. Jin, and Z. Du, “Low-cost reconfigurable 1 bit millimeter-wave array antenna for mobile terminals,” *IEEE Transactions on Antennas and Propagation*, vol. 70, no. 6, pp. 4507–4517, 2022.

[8] M. Abdollahvand, K. Forooraghi, Z. Atlasbaf, E. Martinez-de Rioja, J. A. Encinar, A. Ebrahimi, and S. Ghosh, “Reconfigurable fss based on pin diodes for shared-aperture x/ka-band antennas,” in *2021 15th European Conference on Antennas and Propagation (EuCAP)*. IEEE, 2021, pp. 1–4.

[9] B. Schoenlinner, A. Abbaspour-Tamijani, L. C. Kempel, and G. M. Rebeiz, “Switchable low-loss rf mems ka-band frequency-selective surface,” *IEEE transactions on microwave theory and techniques*, vol. 52, no. 11, pp. 2474–2481, 2004.

[10] H. Zhang, B. Di, L. Song, and Z. Han, *Reconfigurable Intelligent Surface-Empowered 6G*. Springer, 2021.

[11] Y. Liu, X. Liu, X. Mu, T. Hou, J. Xu, M. Di Renzo, and N. Al-Dhahir, “Reconfigurable intelligent surfaces: Principles and opportunities,” *IEEE communications surveys & tutorials*, vol. 23, no. 3, pp. 1546–1577, 2021.

[12] N. Ojaroudi Parchin, H. Jahanbakhsh Basherlou, Y. I. Al-Yasir, A. M. Abdulkhaleq, and R. A. Abd-Alhameed, “Reconfigurable antennas: Switching techniques—a survey,” *Electronics*, vol. 9, no. 2, p. 336, 2020.

[13] W. Disharoon, S. Y. Lee, J. Ramsey, and N. Ghalichechian, “Overview of reconfiguration technologies for reflectarrays and trasmitarrays,” in *2023 17th European Conference on Antennas and Propagation (EuCAP)*. IEEE, 2023, pp. 1–5.

[14] Y.-H. Cho and G. M. Rebeiz, “Two-and four-pole tunable 0.7–1.1-ghz bandpass-to-bandstop filters with bandwidth control,” *IEEE Transactions on Microwave Theory and Techniques*, vol. 62, no. 3, pp. 457–463, 2014.

[15] B. D. Nguyen and C. Pichot, “Unit-cell loaded with pin diodes for 1-bit linearly polarized reconfigurable transmitarrays,” *IEEE Antennas and Wireless Propagation Letters*, vol. 18, no. 1, pp. 98–102, 2018.

[16] S. Ojaroudi, Y. Ojaroudi, and N. Ojaroudi, “Novel design of reconfigurable microstrip slot antenna with switchable band-notched characteristic,” *Microwave and Optical Technology Letters*, vol. 57, no. 4, pp. 849–853, 2015.

[17] J. Wang, W. Tang, J. C. Liang, L. Zhang, J. Y. Dai, X. Li, S. Jin, Q. Cheng, and T. J. Cui, “Reconfigurable intelligent surface: Power consumption modeling and practical measurement validation,” *arXiv preprint arXiv:2211.00323*, 2022.

[18] A. Javed, B. Bhellar, and F. A. Tahir, “Reconfigurable body worn antenna for bluetooth and wimax,” in *2015 12th International Bhurban Conference on Applied Sciences and Technology (IBCAST)*, 2015, pp. 571–573.

[19] H. S. Munawar, “An overview of reconfigurable antennas for wireless body area networks and possible future prospects,” *Int. J. Wirel. Microw. Technol*, vol. 10, no. 2, pp. 1–8, 2020.

[20] M. Di Renzo, A. Zappone, M. Debbah, M.-S. Alouini, C. Yuen, J. De Rosny, and S. Tretyakov, “Smart radio environments empowered by reconfigurable intelligent surfaces: How it works, state of research, and the road ahead,” *IEEE journal on selected areas in communications*, vol. 38, no. 11, pp. 2450–2525, 2020.

[21] D. Dobkin, *The rf in RFID: uhf RFID in practice*. Newnes, 2012.

[22] “Em4152 datasheet.” [Online]. Available: https://www.emmicroelectronic.com/sites/default/files/products/datasheets/4152-DS%20v4.2.pdf

[23] “Em4325 datasheet.” [Online]. Available: https://www.emmicroelectronic.com/sites/default/files/products/datasheets/4325-DS%20%28updated%20datasheet%20Feb%202023%29.pdf

[24] E. Pantoja, R. Sreekumar, S. Mosanu, T. Tracy, and M. Stan, “Virtualized controller for computational rfid-based iot sensors,” in *2023 IEEE International Conference on RFID (RFID)*, 2023, pp. 54–59.

[25] A. Mostaccio, S. Amendola, N. D. C. Occhiuzzi, E. Martinelli, and G. Marrocco, “Ultra-low power rfid-based wake-up architectures for wireless sensor networks in industrial plants,” in *2023 IEEE 13th International Conference on RFID Technology and Applications (RFID-TA)*, 2023, pp. 146–149.

[26] I. Vardakis, G. Kotridis, S. Peppas, K. Skyvalakis, G. Vougioukas, and A. Bletsas, “Intelligently wireless batteryless rf-powered reconfigurable surface,” in *2021 IEEE Global Communications Conference (GLOBECOM)*. IEEE, 2021, pp. 1–6.

[27] Z. X. Wang, C. K. Shen, J. W. Wu, H. Xu, Q. Cheng, T. T. Ye, and T. J. Cui, “A long-range and nearly passive rfid-controlled information metasurface,” *Advanced Optical Materials*, vol. 12, no. 6, p. 2203114, 2024. [Online]. Available: https://onlinelibrary.wiley.com/doi/abs/10.1002/adom.202203114

[28] F. Lestini, G. Marrocco, and C. Occhiuzzi, “Feasibility of rfid-based control of reconfigurable intelligent surfaces (riss) for wireless communication systems,” in *2023 IEEE 13th International Conference on RFID Technology and Applications (RFID-TA)*. IEEE, 2023, pp. 241–244.

[29] “EPC Radio-Frequency Identity Protocols Generation 2 UHF RFID Standard.” [Online]. Available: https://www.gs1.org/sites/default/files/docs/epc/gs1-epc-gen2v2-uhf-airinterfacei21r2018-09-04.pdf

[30] A. Sample and J. R. Smith, “Experimental results with two wireless power transfer systems,” in *2009 IEEE radio and wireless symposium*. IEEE, 2009, pp. 16–18.

[31] F. Muralter, M. Hani, H. Landaluce, A. Perallos, and E. Biebl, “Uhf rfid chip impedance and sensitivity measurement using a transmission line transformer,” in *2021 IEEE International Conference on RFID (RFID)*. IEEE, 2021, pp. 1–4.

[32] "Mini-Circuits TCM1-83X+ 1:1 CORE and WIRE Transformer." [Online]. Available: https://www.minicircuits.com/WebStore/dashboard.html?model=TCM1-83X%2B
[33] R. Kronberger, A. Geissler, and B. Friedmann, "New methods to determine the impedance of uhf rfid chips," in *2010 IEEE International Conference on RFID (IEEE RFID 2010)*. IEEE, 2010, pp. 260–265.
[34] "PicoVNA108 Vector Network Analyzer." [Online]. Available: https://www.picotech.com/vector-network-analyzer/picovna/picovna-series
[35] G. Marrocco, "The art of uhf rfid antenna design: Impedance-matching and size-reduction techniques," *IEEE antennas and propagation magazine*, vol. 50, no. 1, pp. 66–79, 2008.
[36] M. Schink, A. Wagner, F. Unterstein, and J. Heyszl, "Security and trust in open source security tokens," *IACR Transactions on Cryptographic Hardware and Embedded Systems*, pp. 176–201, 2021.
[37] "Magnus-s3 datasheet." [Online]. Available: https://www.axzon.com/packagedQFN.html
[38] "Skyworks SMP1322 Series PIN diode." [Online]. Available: https://www.skyworksinc.com/-/media/SkyWorks/Documents/Products/101-200/SMP1322_Series_200049W.pdf
[39] "Ferrite beads datasheet." [Online]. Available: https://www.murata.com/en-us/products/productdata/8800880459806/ENFJ0016.pdf
[40] "7 Series FPGAs Data Sheet: Overview." [Online]. Available: https://www.mouser.com/datasheet/2/903/ds180_7Series_Overview-1591537.pdf

Francesco Lestini (Student Member, IEEE) was born in Genzano di Roma, Italy, in 1997. He received the B.S. and M.S. degrees (Hons.) in medical engineering in 2019 and 2021, respectively, from the University of Rome Tor Vergata, Rome, Italy, where he is currently pursuing the Ph.D. degree in computer science, control and geoinformation with the Pervasive Electromagnetics Lab. Since 2023, he has been a part-time R&D RF Engineer with RADIO6ENSE Srl. His research focuses on the wireless reconfigurability of electromagnetic devices through RFID technology and on developing epidermal RFID grids for distributed skin temperature measurement. Mr. Lestini is also part of the Cyber4Health observatory, which focuses on raising international awareness about the need for pre-market regulations related to medical devices' Cyber and Physical security. He received the Best Paper Award at the 7th edition of SpliTech Conference (2022) on Smart and Sustainable Technologies and an Honorary Mention by URSI for the Young Scientist "Roberto Sorrentino" Award (2023).

Gaetano Marrocco (Senior Member, IEEE) is Full Professor of Electromagnetics Engineering at the University of Roma Tor Vergata, where he currently leads the Medical Engineering School. Since 2002, he has been a pioneer in Radiofrequency Identification and Sensing. His current research focuses on wireless-activated sensors, Wearable and Epidermal Electronics, and structural antennas for sensorized skins, smart prostheses, and finger augmentation devices for Tactile Internet. He serves as an Associate Editor of the IEEE Journal of Radiofrequency Identification and track Editor of the IEEE Journal of Flexible Electronics. Additionally, he chairs the Italian Section of URSI Commission D Electronics and Photonics and is a co-founder and president of the University spin-off RADIO6ENSE. RADIO6ENSE is actively involved in short-range electromagnetic sensing for Industrial Internet of Things, Smart Manufacturing, Automotive, and Digital Health. He is also listed in the PLOS 2022 ranking of the Top 2 % Scientists Worldwide.

Cecilia Occhiuzzi (Member, IEEE) received the M.Sc. degree in medical engineering and the PhD from the University of Rome "Tor Vergata.". She is an Associate Professor at the same University, where she teaches Electromagnetic Fields, Biomedical Interaction, and Instrumentation and Techniques for health monitoring and therapy. She is also Co-Founder and CEO of RADIO6ENSE, a spin-off of the University of Tor Vergata active in RFID solutions for the industrial sector. Her research interests include wireless health monitoring through wearable and implantable radiofrequency/mm-wave identification techniques and pervasive sensing paradigms for the food sector and Industry 4.0. She co-authored more than eighty papers in international journals and conferences and ten patents on RFID sensing systems.